Indian Journal of Radio & Space Physics
Vol 44, June 2015, pp 69-77

Kinetic Alfven wave with loss-cone distribution function in the presence of beam velocities in an inhomogeneous magnetosphere

A K Dwivedi[1,$,*], Sunil Kumar[1,#] & M S Tiwari[2,!]

[1]Department of Physics, Harish Chandra P G College, Varanasi 221 001, India

[2]Department of Physics, Dr H S Gour University, Sagar 470 003, India

E-mail: [$]akdwiv@yahoo.co.in; [#]sk496855@gmail.com; [!]tiwarims@yahoo.co.in

Received 4 November 2014; revised 22 May 2015; accepted 27 May 2015

Kinetic Alfven waves in the presence of an inhomogeneous electric field applied perpendicular to the ambient magnetic field with loss-cone distribution function and ion and electron beam are investigated. The particle aspect approach is adopted to investigate the trajectories of charged particles in the electromagnetic field of a kinetic Alfven wave. Expressions are found for the field-aligned current, the perpendicular current and the dispersion relation. The growth/damping rate of the wave is obtained by an energy conservation method. The effect of electron and ion beam, steepness of loss-cone and inhomogeneity of electric field are discussed. The plasma under consideration is assumed to be anisotropic and with low β. The results are interpreted for the space plasma parameter appropriate to the auroral acceleration region of the earth's magnetosphere.

Keywords: Kinetic Alfven wave, Electric field inhomogeneity, Loss-cone distribution function, Auroral current

PACS Nos: 94.30.Cq; 94.30.Kq; *94.30.vb*

1 Introduction

Kinetic Alfven waves are of great importance in laboratory and space plasmas. These waves play an important role in energy transport, in driving field-aligned currents, in particle acceleration and heating, and in explaining inverted-V structures in magnetosphere–ionosphere coupling and in solar flares and the solar wind[1-3]. The magnetohydrodynamic (MHD) Alfven wave is converted to kinetic Alfven waves via the ion finite Larmor radius effect[1,4]. Kinetic Alfven waves are accompanied by a compressive magnetic field and a parallel electric field. Kinetic Alfven waves have been implicated in a wide variety of geophysical processes from the ionosphere to the solar corona[5,6]. Observations of electric fields in the ionosphere and the magnetosphere using various techniques have led to important advances in the understanding of magnetosphere-ionosphere coupling. The plasma sheet plays an important role in the transfer of energy and matter from the solar wind to the ionosphere[7]. The kinetic Alfven waves are accompanied by the electric field along the background magnetic field and can accelerate and heat charged particles[8].

Electric fields of the order of hundreds of milli volts per meter have been predicted in the high latitude ionosphere, the auroral zone, magnetotail and the plasma sheet[9-14]. In a variety of situations, in particular at the time of sub-storm onset, the interplanetary magnetic field reverses its direction and two oppositely directed inhomogeneous electric fields are reported in the plasma sheet and in the auroral zone[9,10]. Over the last decade, it has been established that auroral luminosity is due to the impact of an accelerated electron beam coming towards the ionosphere and at the same event, the upcoming ion beam has also been observed towards the magnetotail[15,16]. In the recent past, particle aspect analysis was used to explain the auroral particle acceleration in terms of Alfven waves and kinetic Alfven waves propagating parallel to or obliquely with respect to the ambient magnetic field[14,17-20].

The purpose of this paper is to investigate the effect of ion and electron beams on the kinetic Alfven waves in the presence of loss-cone distribution function and an inhomogeneous electric field in the auroral region by using particle aspect analysis. The theory is based on Dawson's theory of Landau damping, which was further extended by Terashima[21], Tiwari *et al.*[22], Varma & Tiwari[23], Baronia & Tiwari[14,17] and Dwivedi *et al.*[18-20] for the analysis of electrostatic and electromagnetic waves. The advantage of this approach is its suitability for dealing with auroral electrodynamics and energy exchange by wave-particle resonant interaction.

2 Basic assumptions

In this model, the plasma is divided into two groups of particles: resonant and non-resonant. It is supposed that resonant electrons participate in the energy exchange with waves, whereas non-resonant particles support the oscillatory nature of the waves. A wave propagating obliquely to the magnetic field in a plane normal to the density gradient and applied electric field is considered, in anisotropic plasma. The ambient magnetic field is directed along the z-axis, and the density gradient and perpendicular electric field are in the y-direction. The wave is propagating in the (x, z) plane.

The kinetic Alfven wave is assumed to originate at t = 0 when the resonant particles are undisturbed. The low β (ratio of plasma pressure to the magnetic pressure) is considered collision-less plasma satisfying the conditions:

$$V_{T\|i} << \frac{\omega}{k_\|} << V_{T\|e};\ \omega << \Omega_i, \Omega_e;\ k_\perp^2 \rho_e^2 << k_\perp^2 \rho_i^2 < 1 \quad \ldots (1)$$

where, $V_{T\|i}$ and $V_{T\|e}$, are the thermal velocities of ions and electrons along the magnetic field; $\Omega_{i,e}$, gyration frequencies; ω, the wave frequency; and $\rho_{i,e}$, the mean gyro-radii of the respective species. $k_\perp$ and $k_\|$ define the components of wave vector $\overline{k}$ perpendicular and parallel to the magnetic field B_0.

Consider a kinetic Alfven wave of the form[14,17-19]:

$$E = E_\perp + E_\|. \quad \ldots (2)$$

where,

$$E_\perp = -\nabla_\perp \phi,\ E_\| = -\nabla_\| \psi$$

and

$$\phi = \phi_1 \cos(k_\perp x + k_\| z - \omega t) \quad \ldots (3a)$$

$$\psi = \psi_1 \cos(k_\perp x + k_\| z - \omega t) \quad \ldots (3b)$$

where, ϕ_1 and ψ_1, are assumed to be a slowly varying function of time t. Electrons streaming with their thermal velocity along the field lines are assumed to interact with the electric field of the kinetic Alfven wave. Electrons whose velocity is slightly less than the parallel phase velocity $\omega/k_\|$ of the wave cause Landau damping of the wave. The inhomogeneous applied electric field $E_{(y)}$ has the form of a stable mode, and is given as[14]:

$$E_{(y)} = E_0\left(1 - \frac{y^2}{a^2}\right)$$

where, a, is taken to be comparable to the mean ion gyroradius but much larger than the Debye length. When, $y^2/a^2 << 1$, $E_{(y)}$ becomes a constant uniform field. In the case, y > a, the electric field changes sign and is oppositely directed.

3 Distribution function

The perturbed density is adopted for non-resonant particles in the presence of the kinetic Alfven wave for the inhomogeneous plasma[14]. To determine the dispersion relation and the associated currents, the distribution function of the form[18] is used:

$$N(y,\bar{V}) = N_0[1 - \varepsilon(y + \frac{V_x}{\Omega})] f_\perp(V_\perp) f_\|(V_\|) \quad \ldots (4)$$

where,

$$f_\perp(V_\perp) = \frac{V_\perp^{2J}}{\pi V_{T_\perp}^{2(J+1)} J!} \exp\{-V_\perp^2 / V_{T\perp}^2\} \quad \ldots (5)$$

$$f_\|(V_\|) = \left(\frac{1}{\pi V_{T\|}}\right) \exp\left\{-m\left(V_\| - V_{Dj}\right)^2 / 2T_\|\right\} \quad \ldots (6)$$

where, ε, is a small-scale parameter of the order of inverse of the density gradient scale length. V_{Dj} defines the beam velocity of the particles. Here, m, is the mass; $V_\perp$ and $V_\|$, are the velocities, and $T_\perp$ and $T_\|$, are the temperatures of charged particles perpendicular and parallel to the magnetic field B_0 which is directed along the z-axis. J defines steepness of loss-cone. The wave is propagating in x-z plane normal to density gradient which is along the y-axis.

4 Dispersion relation

The integrated perturbed density for non-resonant particles $n_{i,e}$ is given as:

$$n_{i,e} = \int_0^\infty 2\pi V_\perp dV_\perp \int_{-\infty}^{\infty} dV_\| n_1(r,t) \quad \ldots (7)$$

The expression of n_1 is used for non-resonant particles, which has been evaluated by Baronia & Tiwari[14] as:

$$n_1(\mathrm{r,t}) = N(V)\sum_{-\infty}^{\infty} J_n(\mu)\sum_{-\infty}^{\infty} J_l(\mu)\frac{q}{m}$$

$$\left[\begin{array}{l}\left\{\phi_l - \dfrac{V_{\parallel}k_{\parallel}}{\omega}(\phi_l - \psi_l)\right\}\times \\ \left\{\dfrac{k_\perp^2}{\mathrm{a}_n^2} - \dfrac{\Omega^2 V_d^j k_\perp m}{\Lambda_n \mathrm{a}_n^2 T_\perp}\right\} + \dfrac{k_\parallel^2}{\Lambda_n^2}\psi_1\end{array}\right]\cos\xi_{nl} \quad \text{... (8)}$$

V_d^j is the diamagnetic drift velocity, which is defined by:

$$V_d^j = \frac{T_\perp}{m\Omega}\frac{1}{N}\frac{\partial N}{\partial y} \quad \text{... (9)}$$

and $V_d^j = 0$, represents the homogeneous plasma; q, is the charge, which is equal to e for ions and –e for electrons.

$$\mu = \frac{k_\perp V_\perp}{\Omega}\left[1 + \frac{3}{4}\frac{\tilde{E}'(y)}{\Omega^2}\right]$$

$$\Lambda_n = k_\parallel V_\parallel - \omega + n\Omega + k_\perp\tilde{\Delta}$$

$$\tilde{\Delta} = -\frac{\tilde{E}(y)}{\Omega}\left[1 + \frac{E''(y)}{E(y)}\frac{1}{4}\left(\frac{V_\perp}{\Omega}\right)^2 + \ldots\ldots\ldots\ldots\right]$$

$$\mathrm{a}_n^2 = \Lambda_n^2 - \Omega^2$$

$$\xi_{nl} = k_\perp y + k_\parallel z - \omega t + (n - l)(\Omega t - \theta) \quad \text{... (10)}$$

θ is the initial phase of the charged particles, n and l are running symbols and integer. In view of the approximations [Eq. (3)], the dominant contribution comes from the term n = l = 0 as the contributions due to higher n are negligible[21]. The resonant criterion is given by $k_\parallel V_\parallel - \omega + k_\perp\Delta = 0$, which means that the electrons see the wave independent of t in the particles frame. The particles satisfying the above condition are called resonant. J_s are Bessel's functions, which arise from the different periodical variation of charged particle trajectories. The term represented by Bessel's functions show the reduction of the field intensities due to finite gyroradius effect. With the help of Eqs (4 and 8), the average densities are found for inhomogeneous plasma:

$$\bar{n}_i = \frac{\omega_{pi}^2}{4\pi e}\left[-\frac{k_\perp^2\varphi}{\Omega_i^2} + \frac{k_\parallel^2\psi}{\omega_i^2} + \frac{k_\perp V_d^i m_i}{\omega_i T_{\perp i}}\right]\left(1 - \frac{1}{2}k_\perp^2\rho_i^2(J + 1)\right) \quad \text{... (11)}$$

$$\bar{n}_e = \frac{\omega_{pe}^2}{4\pi e V_{T\parallel e}^2}\psi$$

$$\omega_{pi,e}^2 = 4\pi N_0 e^2 / m_{i,e} \quad \text{... (12)}$$

where, $V_{T\parallel e}^2$, is the square of thermal velocity parallel to the ambient magnetic field. V_d^i is the diamagnetic drift velocity of ions. Using the quasi-neutrality condition[14,18,19,24]:

$$\bar{n}_i = \bar{n}_e, \quad \text{... (13)}$$

One gets the relation between ϕ and ψ as:

$$\frac{\phi}{\psi} = -\frac{\Omega_i^2}{k_\perp^2}\left[\frac{\omega_{pe}^2}{\omega_{pi}^2 V_{T\parallel e}^2\left(1 - \frac{1}{2}k_\perp^2\rho_i^2(J + 1)\right)} - \frac{k_\parallel^2}{\omega_i^2}\right]D_d \quad \text{... (14)}$$

Using perturbed ion and electron densities n_i and n_e and Amperes law in parallel direction[18,19,24], one can obtain the relation:

$$\frac{\partial}{\partial z}\nabla_\perp^2(\phi - \psi) = \frac{4\pi}{c^2}\frac{\partial}{\partial t}J_z \quad \text{... (15)}$$

where,

$$J_Z = e\int_0^\infty 2\pi V_\perp dV_\perp \int_{-\infty}^{\infty} dV_\parallel[(N(V)u_z(r,t) + V_\parallel n_l(r,t))_i$$

$$-(N(V)u_z(r,t) + V_\parallel n_l(r,t))_e] \quad \text{... (16)}$$

u_z(r,t) is the perturbed velocity of charged particles in the presence of a kinetic Alfven wave. J_Z is the current density, which involves first-order perturbations of density and velocity. The expression for u_z (r, t) is calculated by Baronia & Tiwari[14], which is given as:

$$u_z(r,t) = -\frac{q}{m}\left[\psi_l k_\parallel + \frac{V_\perp k_\parallel k_\perp}{\omega}(\phi_l - \psi_l)\frac{n}{\mu}\right]\sum_{-\infty}^{\infty} J_n(\mu)\sum_{-\infty}^{\infty} J_l(\mu) \times \frac{1}{\Lambda_n}[\cos\xi_{nl} - \eta\cos(\xi_{nl} - \Lambda_n t)] \quad \text{... (17)}$$

where, η = 0 for the non-resonant particles and η = 1 for the resonant one. In the analysis, it is assumed that the plasma consist of non-resonant and resonant particles. The non-resonant particles support the oscillatory motion of the wave, whereas the resonant particles participate in energy exchange with the wave. To distinguish the non-resonant and resonant particles, the symbol η = 0 is adopted for non-resonant particles and η = 1 for the resonant particles[21]. The methodology of this paper is based upon the particle aspect analysis[21], which is focused to evaluate the particle trajectories in the presence of wave electromagnetic fields.

With the help of Eqs (14 and 15), one can obtain the dispersion relation for the kinetic Alfven wave in inhomogeneous plasma as:

$$\left(1 - \frac{\omega_i^2}{k_\parallel^2 c_s^2 A}\right)\left(1 - \frac{\omega^2 A}{k_\parallel^2 v_A^2} D_d\right) + \frac{(\omega - k_\parallel V_{De})\omega_{iE} A}{k_\parallel^2 v_A^2} D_d = \frac{k_\perp^2 \omega^2}{k_\parallel^2 \Omega_i^2} D_d - \left(\frac{\omega_{pe}^2}{\omega_{pi}^2 V_{T\parallel e}^2 A} - \frac{k_\parallel^2}{\omega_i^2}\right) \times A\left(\frac{\omega_{pi}^2 \omega_i^2 T_{\parallel i}}{c^2 \Omega_i^2 k_\parallel^2 m_i} - \frac{V_d^i k_\perp m_i \omega_{pi}^2 \omega_i^2 A}{T_{\perp i} c^2 k_\parallel^3 k_\perp^2}\right) \quad \text{... (18)}$$

where,

$$D_d = \left(1 - \frac{V_d^i k_\perp \Omega_i^2 m_i}{T_{\perp i} k_\perp^2 \omega_i}\right); \quad A = \left(1 - \frac{1}{2} k_\perp^2 \rho_i^2 (J+1)\right)$$

$$\omega_i = \omega - \omega_{iE} - k_\parallel V_{Di}; \quad \omega_{iE} = \omega_E (1 - \delta)$$

$$\delta = \frac{\rho_i^2}{2a^2}; \quad \omega_E = \frac{k_\perp E_0}{B_0}$$

where,

$$c_s^2 = \frac{\omega_{pi}^2 V_{T\parallel e}^2}{\omega_{pe}^2}$$

is the square of ion-acoustic speed and

$$v_A^2 = \frac{c^2 \Omega_i^2}{\omega_{pi}^2}$$

is the square of Alfven speed. The dispersion relation of the kinetic Alfven wave reduces to that derived by Hasegawa & Chen[25], Baronia & Tiwari[14] under the approximation, $V_d^i = 0$, $V_{Di}=0$, $V_{De}=0$ and $I_0(\lambda_i)\exp(-\lambda_i) \sim 1-\lambda_i$, for $\lambda_i = ½\, k_\perp^2 \rho_i^2 < 1$ as it has been applied. $I_0(\lambda_i)$ is the modified Bessel function. δ defines degree of electric field inhomogeneity.

5 Current density

Since the average value of current vanishes, which is contributed by first order perturbations of density and velocity due to their periodical variations, the average current per unit wavelength is evaluated, which is the second order perturbation. To evaluate the perturbed current density per unit wavelength, the following set of equations are used:

$$\bar{J}_{i,e} = \int_0^\lambda ds \int_0^\infty 2\pi V_\perp dV_\perp \int_{-\infty}^\infty dV_\parallel e\left[(N + n_i)(\bar{V} + \bar{u}) - N\bar{V}\right]_{i,e} \quad \text{... (19)}$$

and $\bar{J} = \bar{J}_i - \bar{J}_e$ ... (20)

With the help of Eqs (4, 8 and 17), following relations are obtained:

$$J_X = \frac{\psi_l e k_\perp k_\parallel^2 \lambda}{8\pi}\left[\frac{\omega_{pe}^2}{m_e \Omega_e^2}\left\{\left(\frac{\phi_l - \psi_l}{\omega}\right)\left(1 - \frac{2\omega_e^2}{k_\parallel^2 V_{T\parallel e}^2}\right) + \frac{2\omega_e}{k_\parallel^2 V_{T\parallel e}^2}\phi_l\right\} - \frac{\omega_{pi}^2\left(1 - k_\perp^2 \rho_i^2 (J+1)\right)\phi_l}{m_i \Omega_i^2 \omega_i}\right] \quad \text{... (21)}$$

$$J_Z = \frac{e\psi_l k_\parallel \lambda}{8\pi}\left[\frac{\omega_{pe}^2}{m_e}\left\{\frac{k_\perp^2}{\Omega_e^2}\left\{\left(\frac{\phi_l - \psi_l}{\omega}\right) + \frac{2\omega_e \psi_l}{k_\parallel^2 V_{T\parallel e}^2}\right\} - \frac{8\omega_e}{k_\parallel^2 V_{T\parallel e}^4}\psi_l\right\} - \frac{\omega_{pi}^2}{m_i}\left\{\frac{k_\perp^2}{\Omega_i^2 \omega_i}\phi_l - \frac{4\psi_l}{k_\parallel V_{T\parallel i}^2} + \frac{4\psi_l}{V_{T\parallel i}^2 \omega_i}\right\}\left(1 - k_\perp^2 \rho_i^2 (J+1)\right)\right] \quad \text{... (22)}$$

where,

$$\omega_e = \omega - \omega_{iE} - k_\parallel V_{De}$$

In the evaluation of the current densities, it was assumed that the field-aligned and perpendicular currents are due to an electromagnetic kinetic Alfven wave and the contribution due to diamagnetic drift was very less and neglected.

6 Growth / Damping rate

Evaluating the wave energy density per unit wavelength and changes in energy of non-resonant and resonant particles, Terashima[21], Varma & Tiwari[23] and Dwivedi *et al.*[18,19] have derived the growth/damping rate by performing a considerable amount of algebraic calculations, which is of the form:

$$\gamma = (1/\psi_1)(d\psi_1/dt)$$

$$\gamma = A\omega(T_{\parallel e}/m_e)\left\{\frac{k_\perp V_d^e}{k_\parallel (T_{\parallel e}/m_e)} f_{\parallel e}(\omega/k_\parallel) + f'_{\parallel e}(\omega/k_\parallel)^3\right\} \quad \text{... (23)}$$

Substituting Eq. (6), the growth/damping rate is finally obtained as:

$$\gamma/\omega = \pi^{1/2}\frac{\omega_e^2}{\omega k_\parallel V_{T\parallel e}}\left(\frac{T_{\parallel e}k_\perp V_d^e}{T_{\perp e}\omega_e} - 1\right)\exp\left[-\frac{\omega_e^2}{k_\parallel^2 V_{T\parallel e}^2}\right] \quad \text{... (24)}$$

where, $V_{T\perp,\parallel}^2 = (2T_{\perp,\parallel}/m)$; V_d^e represents electron diamagnetic drift velocity and the value of ω for the drift kinetic Alfven wave has to be submitted. In case of $V_{De} = 0$, the growth rate is recovered as derived by Dwivedi *et al.*[18,19] and Baronia & Tiwari[14,17]. The kinetic Alfven waves are generated by density inhomogeneity if the electric field inhomogeneity is absent. However, due to the electric field inhomogeneity, the condition is altered.

7 Results and Discussion

In the numerical evaluation of the growth rate, current and dispersion, the following parameters are used for the auroral acceleration region[14,15,17-20]:

B_0 =4300 nT, Ω_i =412 s^{-1}, $KT_{\parallel i}$ =1 keV,

$KT_{\parallel e}$ = 10 keV, $V_d^e = 200$ cm s^{-1}, ω_{pi}/Ω_i=10 K

7.1 Dispersion relation

The dispersion relation Eq. (18) has been solved numerically using the Newton-Raphson method and the value of ω are plotted versus $k_\perp\rho_i$ in Fig. 1(a). It is clear that the wave frequency (ω) increases with increase of the applied electric field. The wave frequency (ω) is slightly decreasing with increasing value of $k_\perp\rho_i$ under the condition $k_\perp\rho_i$ <1. The wave frequency is dependent on $k_\perp\rho_i$; the nature of wave is different, when $k_\perp\rho_i$ <1; and for $k_\perp\rho_i$ >1, wave frequency increases as $k_\perp\rho_i$ increases. The effect of electric field inhomogeneity (δ) and distribution index (J) on wave frequency is depicted in Figs [1(b) and 2(a)]. The wave frequency decreases with increasing degree of inhomogeneity and distribution

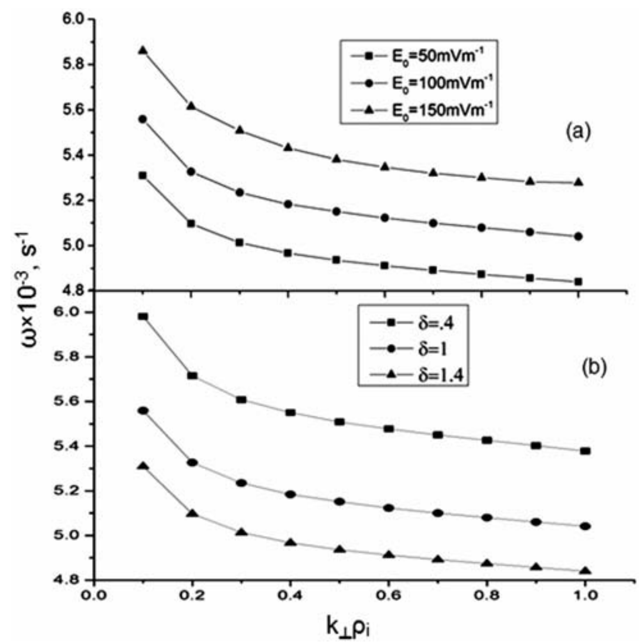

Fig. 1 — Frequency (ω) versus perpendicular wave number ($k_\perp\rho_i$) for different: (a) E_0; and (b) δ [V_{Di} = - 4×10^5 cm s^{-1}; V_{De} = 1× 10^7 cm s^{-1}; J = 2]

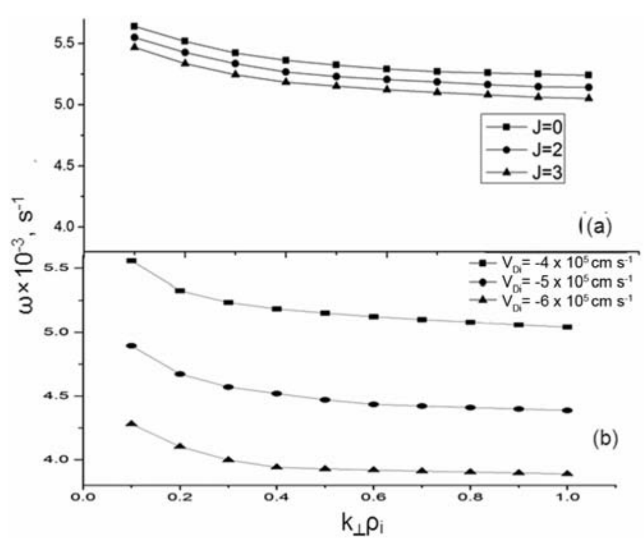

Fig. 2 — Frequency (ω) versus perpendicular wave number ($k_\perp\rho_i$) for different: (a) J; and (b) V_{Di} [V_{De} = 1×10^7 cm s^{-1}; E_0 = 100 mV m^{-1}; δ = 1.0]

index J. The wave frequency, ω, decreases with the distribution index, J, may be due to the decrease of ion drift velocity by averaging the wave field over the Larmor orbit in the presence of steep loss-cone distribution functions. Wave frequency decreases with increase of $k_\perp\rho_i$. Figure 2(b) shows the variation of wave frequency ω with $k_\perp\rho_i$ for different value of ion beam velocities. It is observed that wave frequency decreases with increase of ion beam velocities.

7.2 Growth / Damping rate

Figures 3(a and b) show the variation of growth/damping rate with $k_\perp\rho_i$ for different value of electric field and electric field inhomogeneity, respectively. It is observed that electric field decreases the growth/damping rate, whereas electric field inhomogeneity, δ, increases the growth/damping rate. It is also found that wave is damped at lower $k_\perp\rho_i$ while excited at higher $k_\perp\rho_i$. Electric field and electric field inhomogeneity are more effective at higher $k_\perp\rho_i$. Figure 4(a) shows the effect of distribution index on growth/damping rate. It is observed that distribution index enhances the growth rate and permit low frequency waves for emission. Figures [4(b) and 5] show the variation of growth/damping rate with $k_\perp\rho_i$ for different values of ion and electron beam velocities. It is observed that both ion and electron beam velocities enhance the growth/damping rate.

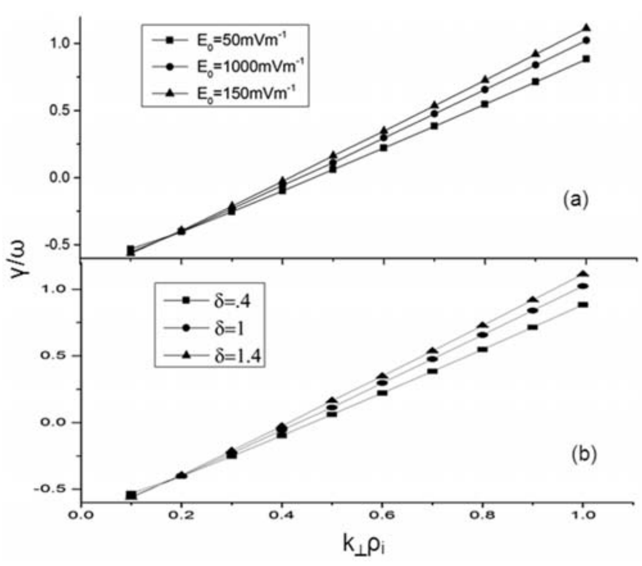

Fig. 3 — Growth/damping rate (γ/ω) versus perpendicular wave number ($k_\perp\rho_i$) for different: (a) E_0; and (b) δ [V_{Di} = - 4× 10^5 cm s^{-1}; V_{De} = 1×10^7 cm s^{-1}; J = 2]

7.3 Electric current

The effect of electric field and electric field inhomogeneity on parallel current is shown in Figs 6(a and b). The electric field increases the parallel current, whereas electric field inhomogeneity decreases the parallel current. The distribution index, J, decreases the parallel current as shown in Fig. 7(a). Figures [7(b) and 8] show the variation of parallel current with $k_\perp\rho_i$ for different value of ion and electron beam velocity. It is seen that both ion and electron beam velocities decrease the parallel current. It is seen that J_z change sign at higher value of $k_\perp\rho_i$ and its magnitude is decreasing. Thus, the magnitude of the field-aligned current may depend upon the perpendicular wave number and the ion gyro-radius. Figures 9(a and b) show the variation of the perpendicular current with $k_\perp\rho_i$ for different values of electric field and electric field

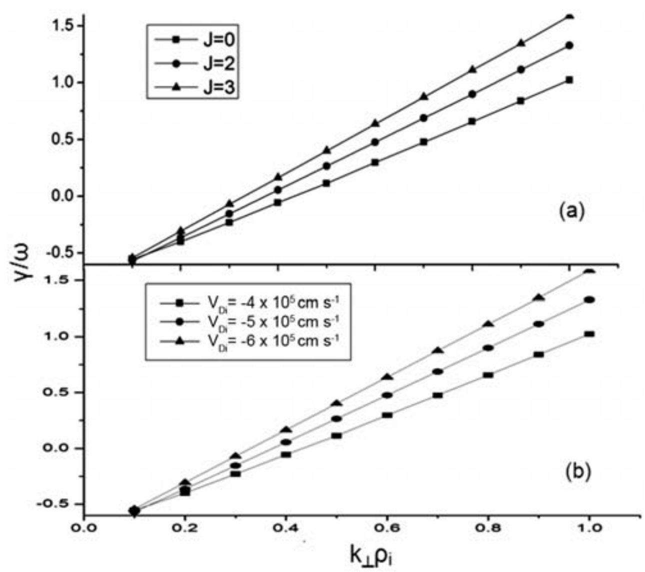

Fig. 4 — Growth/damping rate (γ/ω) versus perpendicular wave number ($k_\perp\rho_i$) for different: (a) J; and (b) V_{Di} [V_{De} = 1×10^7 cm s^{-1}; E_0 = 100 mV m^{-1}; δ = 1.0]

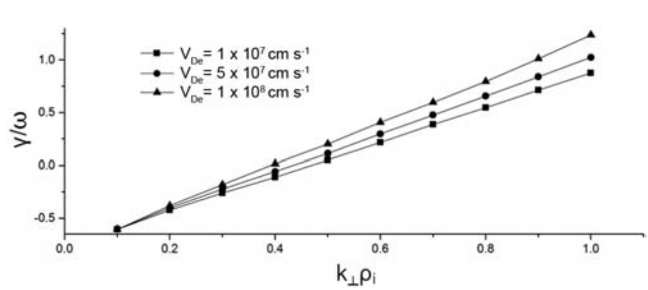

Fig. 5 — Growth/damping rate (γ/ω) versus perpendicular wave number ($k_\perp\rho_i$) for different electron beam velocity V_{De} [V_{Di} = - 4×10^5 cm s^{-1}; E_0 = 100 mV m^{-1}; δ = 1.0; J = 2]

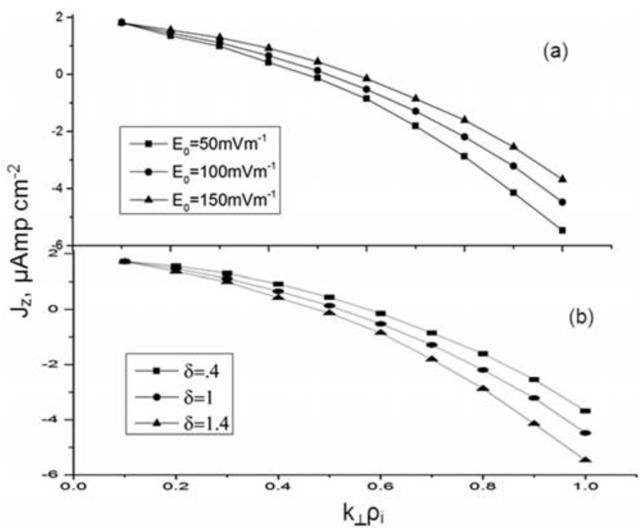

Fig. 6 — Parallel current (J_Z) versus perpendicular wave number ($k_\perp\rho_i$) for different: (a) E_0; and (b) δ [V_{Di} = - 4×10^5 cm s^{-1}; V_{De} = 1×10^7 cm s^{-1}; J = 2]

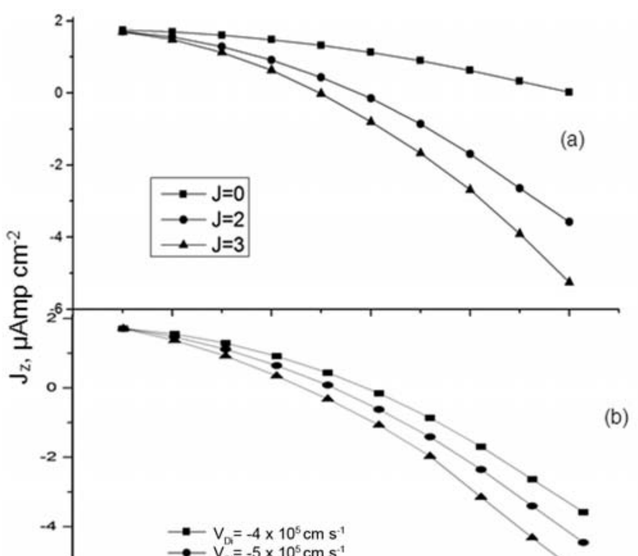

Fig. 7 — Parallel current (J_Z) versus perpendicular wave number ($k_\perp\rho_i$) for different: (a) J; and (b) V_{Di} [V_{De} = 1×10^7 cm s^{-1}; E_0 = 100 mV m^{-1}; δ = 1.0]

inhomogeneity. It is observed that electric field enhance the perpendicular current, whereas electric field inhomogeneity reduces the perpendicular current. Figure 10(a) shows that the perpendicular current decreases with the increase of distribution index, J, for $k_\perp\rho_i$ less than 0.7. The effect of ion and electron beam velocity on perpendicular current are

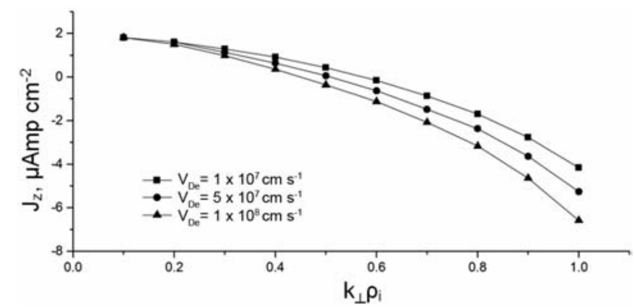

Fig. 8 — Parallel current (J_Z) versus perpendicular wave number ($k_\perp\rho_i$) for different electron beam velocity V_{De} [V_{Di} = - 4×10^5 cm s^{-1}; E_0 = 100 mV m^{-1}; δ = 1.0; J = 2]

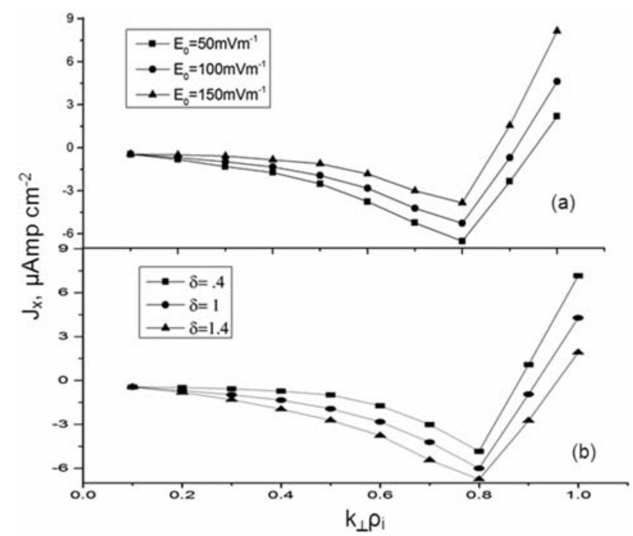

Fig. 9 — Perpendicular current (J_X) versus perpendicular wave number ($k_\perp\rho_i$) for different: (a) E_0; and (b) δ [V_{Di} = - 4×10^5 cm s^{-1}; V_{De} = 1×10^7 cm s^{-1}; J = 2]

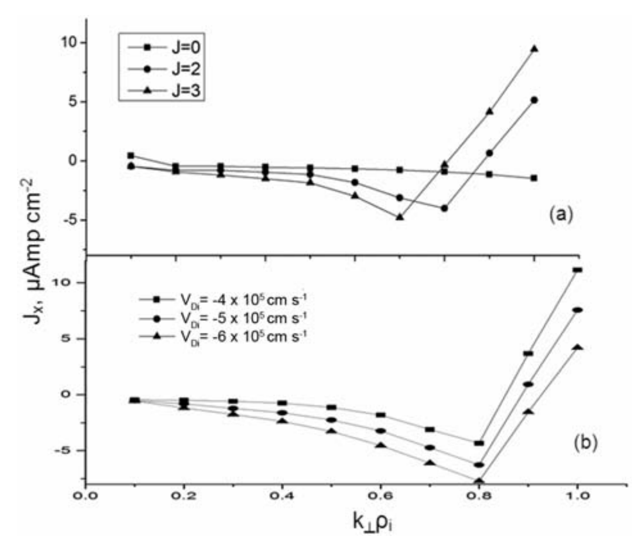

Fig. 10 — Perpendicular current (J_X) versus perpendicular wave number ($k_\perp\rho_i$) for different: (a) J; and (b) V_{Di} [V_{De} = 1×10^7 cm s^{-1}; E_0 = 100 mV m^{-1}; δ = 1.0]

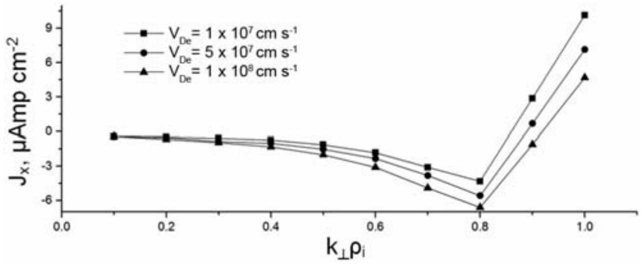

Fig. 11 — Perpendicular current (J_X) versus perpendicular wave number ($k_\perp \rho_i$) for different electron beam velocity V_{De} [V_{Di} = - 4×10^5 cm s^{-1}; E_0 = 100 mV m^{-1}; δ = 1.0; J = 2]

shown in Figs [10(b) and 11]. It is observed that both ion and electron beam velocity decrease the perpendicular current. It is clear from the Figs [9(a) to 11] that the perpendicular currents change sign and its magnitude first decreases up to $k_\perp \rho_i$ ~ 0.8 and then increases but in opposite direction.

8 Conclusion

The present investigation of kinetic Alfven wave incorporates the effectiveness of electric field inhomogeneity in the presence of ion and electron beam. The effect of steep loss-cone distribution function, which may be more appropriate for particle distribution due to converging magnetic field lines of the ionosphere, is considered. It is also noticed that electric field inhomogeneity is more effective on parallel current in the presence of distribution index, J, and ion and electron beams as compared to earlier work[14]. It is noticed that ion and electron beam velocities are more effective towards higher $k_\perp \rho_i$ in the presence of inhomogeneous electric field as compared to earlier work[26]. The calculated values of frequency are smaller than the observed values 0.1–0.4 Hz. The electric field inhomogeneities support the kinetic Alfven wave generation. The particle aspect analysis adopted here also predict the currents associated with the wave. The kinetic Alfven wave may be generated in the distant magnetosphere either by electric field inhomogeneity[14] or density inhomogeneity[27] at sub-storm times and propagates towards the ionosphere leading to acceleration and current pattern as reported by Freja[28] and FAST satellite data[29].

The ion and electron beams are capable of generating kinetic Alfven waves and the direction of current is controlled by the electron and ion beam velocities. In the past, variety of theories are produced for the development of parallel electric fields on auroral field lines. The present investigation may be useful to explain observed Poynting flux[6] along auroral field lined towards the earth by the large scale Alfvenic waves. The waves generated above the acceleration region are supported by electric field inhomogeneity in the presence of ion and electron beams with distribution index, J, carrying energy towards earth's ionospheric regions to display aurora.

Acknowledgement

Financial assistance by Department of Science and Technology, New Delhi is thankfully acknowledged.

References

1 Hasegawa A & Chen L, Kinetic process of plasma heating due to Alfvén wave excitation, *Phys Rev Lett (USA)*, 35 (1975) 370.

2 Goertz C K & Boswell R W, Magnetosphere – ionosphere coupling, *J Geophys Res (USA),* 84 (1979) 7293.

3 Goertz C K, Kinetic Alfven waves on auroral field lines, *Planet Space Sci (UK),* 32 (1984) 1387.

4 Duan S P, Li Z Y & Liu Z X, Kinetic Alfvén waves driven by the density inhomogeneity in the presence of loss-cone distribution function-particle aspect analysis, *Planet Space Sci (UK),* 53 (2005) 1167.

5 Leamon R J, Smith C W, Ness N F & Wong H K, Dissipation range dynamics: Kinetic Alfvén waves and the importance of βe, *J Geophys Res (USA),* 104 (1999) 22331.

6 Wygant J R, Keiling A, Cattell C A, Lysak R L, Temerin M, Mozer F S, Kletzing C A, Scudder J D, Streltsov V, Lotko W & Russel C T, Evidence for kinetic Alfven waves and parallel electron energization at 4-6R_E altitudes in the plasma sheet boundary layer, *J Geophys Res (USA),* 107 (2002), doi: 10.1029/2001JA900113.

7 Borovsky J, Thomsen M & Elphic R, The driving of the plasma sheet by the solar wind, *J Geophys Res (USA)*, 103 (1998) 17617.

8 Duan S P, Liu Z X & Angelopoulos V, Observations of kinetic Alfven wave by THEMIS near a substorm, *Chinese Sci Bulletin*, 57 (2012) 1429.

9 Mozer F S & Lucht P, The average auroral zone electric field, *J Geophys Res (USA),* 79 (1974) 1001.

10 Candidi M & Orsini, Estimate of the north-south electric field component in the magnetotail low latitude boundary layer, *Geophys Res Lett (USA),* 8 (1980) 637.

11 Cattell C A, Mozer F S, Hones E W Jr, Anderson R R & Sharp R D, ISEE observations of the plasma sheet boundary, plasma sheet, and neutral sheet: 1 Electric field, magnetic field, plasma, and ion composition, *J Geophys Res (USA),* 91 (1986) 5663.

12 Mauk B H & Zenetti L J, Magnetospheric electric fields and currents, *Rev Geophys (USA),* 25 (1987) 541.

13 Providakes J F, Kelley M C & Swartz W E, Radar and optical measurements of ionospheric processes associated

with intense sun auroral electric fields, *J Geophys Res (USA),* 94 (1989) 5350.

14 Baronia A & Tiwari M S, Kinetic Alfven waves in an inhomogeneous anosotropic magnetoplasma in the presence of an inhomogeneous electric field: particle aspect analysis, *J Plasma Phys (UK),* 63 (2000) 311.

15 Tiwari M S & Rostoker G, Field-aligned currents and auroral accelerations by non-linear MHD waves, *Planet Space Sci (UK),* 32 (1984) 1497.

16 Mozer F S, Wygant J R, Boehm M H, Cattell C A & Temerin M, Large electric fields in the magnetosphere, *Space Sci Rev (Netherlands),* 42 (1985) 313.

17 Baronia A & Tiwari M S, Kinetic Alfven wave in the presence of loss-cone distribution function in inhomogeneous magnetoplasma-particle aspect analysis, *Planet Space Sci (UK),* 47 (1999) 1111.

18 Dwivedi A K, Varma P & Tiwari M S, Kinetic Alfven wave in the inhomogeneous magnetosphere and general distribution function, *Planet Space Sci (UK),* 49 (2001) 993.

19 Dwivedi A K, Varma P & Tiwari M S, Ion and electron beam effects on kinetic Alfven waves in an inhomogeneous magnetosphere, *Planet Space Sci (UK)*, 50 (2002) 93.

20 Dwivedi A K, Kumar Sunil & Tiwari M S, Effect of ion and electron beam on kinetic Alfven wave in an inhomogeneous magnetic field, *Astrophys Space Sci (Netherlands),* 350 (2014) 547.

21 Terashima Y, Particle aspect analysis of drift instability, *Prog Theor Phys (Japan),* 37 (1967) 775.

22 Tiwari M S, Pandey R P & Misra K D, Particle aspect analysis of drift wave in the presence of inhomogeneous magnetic field, *J Plasma Phys (UK),* 34 (1985) 163.

23 Varma P & Tiwari M S, Ion and electron beam effects on drift wave instability with different distribution functions-particle aspect analysis, *Phys Scrip (Sweden),* 45 (1992) 275.

24 Hasegawa A, Kinetic properties of Alfven waves, *Proc Indian Acad Sci,* 86A (1977) 151.

25 Hasegawa A & Chen L, Kinetic process in plasma heating by resonance mode conservation of Alfven waves, *Phys Fluids (USA),* 19 (1976) 1924.

26 Shukla N, Mishra R, Varma P & Tiwari M S, Ion and electron beam effects on kinetic Alfven wave with general loss-cone distribution function – kinetic approach, *Plasma Phys Control Fusion (UK)*, 50 (2008) 025001, doi: 10.1099/0741-3335/50/2/025001.

27 Southwood D J & Kivelson M G, An approximate description of field – aligned currents in a planetary magnetic field, *J Geophys Res (USA),* 96 (1991) 67.

28 Louarn P, Wahlund J -E, Chust T, de Feraudy H, Holoback B, Dovner P O, Eriksson A I & Holmgren G, Observation of kinetic Alfve'n waves by the FREJA Spacecraft, *Geophys Res Lett (USA),* 21 (1994) 1887.

29 Chaston C C, Bonnell J W, Peticolas L M, Carlson C W, McFadden J P & Ergun R E, Driven Alfven waves and electron acceleration: a FAST case study, *Geophys Res Lett (USA),* 29 (11) (2002) 1535, doi: 10.1029/2001GL013842.